AMERICAN ACADEMY OF OPHTHALMOLOGY®

Retinal Vascular Fingerprints as Novel Biomarkers for Primary Angle Closure Disease Progression

Jin Wang, MD,[1,2,*] *Shumei Han, MD,*[3,4,*] *Dapeng Mou, MD,*[1] *Xin Tang, MD,*[1] *Danli Shi, PhD,*[5] *Mingguang He, MD,*[5] *Chunyan Guo,*[6] *Ningli Wang, MD, PhD,*[1,2] *Ye Zhang, MD*[1]

Purpose: To evaluate retinal vascular parameters across primary angle-closure disease (PACD) stages and explore their association with glaucomatous optic neuropathy (GON).

Design: A cross-sectional, hospital-based study.

Participants: We enrolled 638 eyes from 425 participants aged ≥40 years with PACD and further classified them into primary angle closure suspect (PACS), primary angle closure (PAC), and primary angle closure glaucoma (PACG) groups.

Methods: Retinal vascular parameters were measured using the Retinal-based Microvascular Health Assessment System and compared between 3 groups. A multivariable logistic mixed effects model was used to identify factors associated with the presence of GON.

Main Outcome Measures: Vessel caliber, tortuosity, complexity, and branching angle parameters.

Results: No significant differences in retinal vascular parameters were found between PACS and PAC groups. Eyes in PACG showed significant vascular changes compared to PACS ($P < 0.05$). Elevated intraocular pressure (odds ratio [OR] = 2.44, $P < 0.001$), reduced arteriolar curve tortuosity (OR = 0.12, $P = 0.002$), arteriolar fractal dimension (OR = 0.08, $P = 0.027$), arteriolar branching angle (OR = 0.16, $P = 0.004$), and asymmetry ratio (OR = 0.10, $P < 0.001$ for artery and OR = 0.25, $P = 0.023$ for vein) were significantly associated with the presence of GON.

Conclusions: Retinal "vascular geometric fingerprints" show significant alterations in eyes with PACG compared to PACS and are independently associated with the presence of GON. These findings offer new insights into the vascular changes in GON, and longitudinal studies are needed to determine their prognostic value and clinical utility in managing PACD.

Financial Disclosure(s): The author(s) have no proprietary or commercial interest in any materials discussed in this article. *Ophthalmology Science 2025;5:100848*

Supplemental material available at www.ophthalmologyscience.org.

Glaucoma is a multifactorial progressive optic neuropathy.[1] Although elevated intraocular pressure (IOP) remains a primary risk factor, mounting evidence suggests that vascular function deficiency plays a crucial role in the development and progression of glaucomatous optic neuropathy (GON).[2–5] Therefore, identifying these underlying vascular mechanisms is essential for understanding the pathogenesis of glaucoma and developing potential targeted therapeutic strategies.

Primary angle-closure disease (PACD) is a valuable model for investigating the relationship between vascular alterations and GON. The International Society of Geographical and Epidemiological Ophthalmology proposed a classification system for PACD, which includes primary angle closure suspect (PACS), primary angle closure (PAC), and primary angle closure glaucoma (PACG).[6] This classification represents the progression from anatomical risk (PACS) to elevated IOP without optic nerve damage (PAC) and, finally, to GON (PACG).[6] This staging system enables systematic examination of vascular changes in relation to IOP elevation and GON development across the disease spectrum.

The assessment of retinal vasculature alterations encompasses vascular caliber and vascular geometric parameters.[7–10] Previous studies have shown that a narrower caliber is associated with GON and reduced retinal nerve fiber layer thickness.[7,11,12] However, research on vascular geometric parameters, such as tortuosity, fractal dimension (FD), and branching angle-related parameters, is relatively limited, especially in eyes with PACD. These parameters can provide valuable insights into the optimality of microcirculation and ocular perfusion levels, reflecting retinal hemodynamics and blood flow regulation.[9,13]

To address this research gap, we conducted a cross-sectional study to examine the retinal vascular parameters,

https://doi.org/10.1016/j.xops.2025.100848
ISSN 2666-9145/25

with a particular focus on geometric parameters, across different stages of PACD using a deep learning–based automated computer-assisted program and explored their associations with GON. We hypothesized that retinal vascular parameters would show more pronounced changes in PACG with established GON, and specific parameters would be independently associated with the presence of GON in PACD, even after controlling for IOP.

Methods

Study Population

This observational, cross-sectional, hospital-based study included patients aged ≥40 years who were diagnosed with PACD and visited the Department of Ophthalmology, Beijing Tongren Hospital, between May 2020 and November 2023. The exclusion criteria were as follows: primary open-angle glaucoma; primary glaucoma with indeterminate angle status; secondary glaucoma; a history of acute PAC; and other concurrent retinal diseases, such as diabetic retinopathy, hypertensive retinopathy, and retinal vascular occlusions. Patients with fundus photographs that could not be used for measurements were also excluded.

The Institutional Review Board of Beijing Tongren Hospital waived the need for informed consent and granted ethical approval for the study protocol (TREC2024-KY064). This study was conducted in accordance with the principles of the Declaration of Helsinki.

Study Examinations

All patients underwent comprehensive and standardized ophthalmic assessment, including presenting visual acuity measurement using logarithm of the minimum angle of resolution 4-m charts, slit-lamp examination, IOP measurement using a Canon TX-20 tonometer (Canon), gonioscopic examination using a 1-mirror Goldmann lens (Ocular Instruments), optical biometry using IOLMaster 700 (V.5, Carl Zeiss Meditec), fundus examination using a 90-D lens, and fundus photography using a 45° digital retinal camera (Canon CR 2, Canon). Other examinations included average keratometry and measurements of central corneal thickness, central anterior chamber depth, lens thickness, and axial length using IOLMaster 700. Additionally, medical histories of diabetes, hypertension, and hyperlipidemia were obtained through standardized patient interviews.

Gonioscopy was performed in the dark at high magnification (×25) by one of 2 observers (J.W. and D.M.). The 2 observers attained a κ of 0.82 for assessing the occludable angle in 30 eyes. Static examination was performed under dim ambient illumination with a shortened slit that did not fall on the pupil. Subsequently, indentation gonioscopy was performed with increased illumination to determine the presence of peripheral anterior synechiae.

PACD Classification and GON Assessment

Patients with PACD were categorized into the PACS, PAC, and PACG groups based on the criteria proposed by the International Society of Geographical and Epidemiological Ophthalmology.[6] Primary angle closure suspect was defined as an eye with an occludable angle (the pigmented posterior trabecular meshwork was not visible on gonioscopy at least 180° in the primary position) and an IOP ≤21 mmHg in the absence of peripheral anterior synechiae or GON. Primary angle closure was defined as PACS plus peripheral anterior synechiae or an IOP >21 mmHg but without GON. Primary angle-closure glaucoma was defined as PAC plus GON/visual field defects.[6] Glaucomatous optic neuropathy was defined as a vertical cup-to-disc ratio ≥0.6 and visible retinal nerve fiber layer defect, with or without the presence of optic disc hemorrhage and vertical cup-to-disc ratio asymmetry ≥0.2 between 2 eyes.

Retinal Vessel Imaging and Geometric Parameter Extraction

Binocular 45° digital fundus stereo photographs centered on the midpoint of the optic disc and the macula were acquired for each participant. The spatial resolution of each image was 3072 × 2048 pixels, and the images were stored without compression prior to analysis.

The images were processed using an automatic computer-assisted program named Retinal-based Microvascular Health Assessment System (v. 1.0; Guangzhou Vision Tech Medical Technology Co., Ltd.) by a single observer (D.S.), blinded to the clinical data.[14] This automated system assesses image quality, generates artery and vein segmentation, and computes global physical and geometric measurements within the standard fundus zone (Fig 1). Four categories of retinal vascular parameters were analyzed: vessel caliber, tortuosity, complexity, and branching angle, with detailed definitions provided in Table S1 (available at www.ophthalmologyscience.org). The Retinal-based Microvascular Health Assessment System has been previously validated with high segmentation accuracy across various eye conditions and image qualities.[14] In our study, we further confirmed measurement reproducibility through correlation coefficient analysis, as demonstrated in Table S2 (available at www.ophthalmologyscience.org).

Statistical Analysis

All statistical analyses were performed using R software (version 4.5.0; R Foundation for Statistical Computing). The 1-sample Kolmogorov–Smirnov test was used to assess the normality of the continuous data. Normally distributed continuous data are presented as means and standard deviations, whereas non-normally distributed numerical data are presented as medians and interquartile ranges. Categorical data are presented as frequencies and percentages.

To account for within-subject correlation from both eyes of some participants, we used linear mixed-effects models when comparing retinal vascular parameters among PACD groups, with diagnosis as a fixed effect and subject identification as a random effect. Post hoc pairwise comparisons were performed using estimated marginal means with Tukey adjustment. Effect sizes (Cohen's d) were calculated for key parameters to assess the clinical relevance of group differences. Following conventional thresholds, $|d| = 0.2$, 0.5, and 0.8 represent small, medium, and large effects, respectively.

Factors associated with GON were identified using mixed-effects logistic regression models to adjust for intereye correlation. Multivariable analysis included variables with $P < 0.05$ in univariable analysis, and multicollinearity was assessed using variance inflation factors. Standardized odds ratios (ORs) per standard deviation increase were reported with 95% confidence intervals (CIs). Model performance was evaluated using the area under the receiver operating characteristic curve and compared with the IOP-only model using DeLong test. Statistical significance was defined as $P < 0.05$.

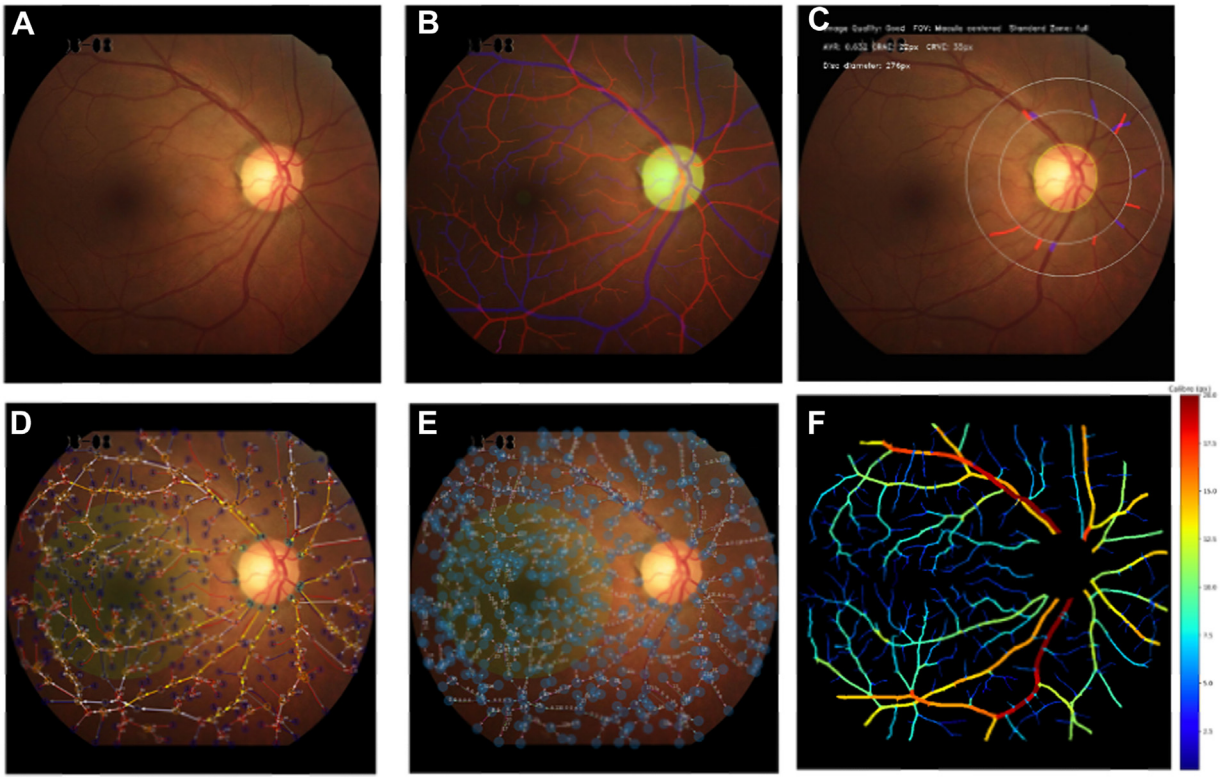

Figure 1. Illustration of RMHAS output. The figure demonstrates the automated analysis of retinal fundus images using the RMHAS. **A**, Original fundus photograph showing the optic disc and retinal vasculature. **B,** Vascular segmentation with arteries (red) and veins (blue) identified. **C,** The measurement range depicted by concentric circles was centered on the optic disc, defining the standard zone for analysis. **D,** Topological map highlighting arterial and venous bifurcations and vessel network complexity. **E,** Curve angle measurement map showing the angles at vessel bifurcations and turns. **F,** Vessel caliber map showing the diameter of retinal vessels using a color scale from blue (smallest) to red (largest). RMHAS = Retina-based Microvascular Health Assessment System.

Results

Demographic and Ocular Characteristics of Study Participants

Of the 968 eyes (484 participants with PACD and completion of all ocular examinations), 330 eyes were excluded based on the following criteria: fundus photographs that were unreadable or could not be used for measurements (146 eyes), intraocular lens implantation with undetermined gonioscopic diagnosis (18 eyes), concurrent retinal diseases (16 eyes with retinal diseases, including retinal vein occlusion, hypertensive retinopathy, diabetic retinopathy, and retinal artery occlusion), and acute PAC (150 eyes). Consequently, a total of 638 eyes (425 participants) were included in the final analysis. A detailed participant selection flowchart is presented in Figure 2.

The study population was categorized into 3 groups—PACS (201 participants, 305 eyes), PAC (57 participants, 91 eyes), and PACG (167 participants, 242 eyes). The demographic and ocular biometric data of the 3 groups are summarized in Table 1. Significant intergroup differences were observed in sex ($P = 0.041$), whereas no differences were noted in the other demographic parameters. Ocular biometric parameters such as presenting visual acuity, IOP, and vertical cup-to-disc ratio differed significantly across the groups (all $P < 0.001$).

Retinal Vessel Parameters across PACD Stages

Table 2 summarizes the distribution of retinal vascular parameters across the 3 diagnostic categories. Histograms of significant vascular parameters are provided in Figure S1 (available at www.ophthalmologyscience.org), illustrating the distributional differences between groups. Comparative analysis revealed no statistically significant differences in any vascular parameters between PACS and PAC groups (all $P > 0.05$).

Significant differences were observed between PACG and PACS groups. For vessel caliber, the PACG group demonstrated higher vascular length-to-diameter ratios (both $P < 0.001$ for artery and vein), with reduced arteriovenous ratio ($P < 0.001$). Regarding vessel tortuosity, eyes with PACG demonstrated decreased arteriolar tortuosity ($P = 0.018$) and curve tortuosity ($P < 0.001$) compared to PACS, whereas venular tortuosity parameters remained unchanged between groups. Fractal dimension, representing vessel complexity, was significantly lower in PACG for both arteries and veins compared to PACS (all $P < 0.001$), indicating reduced vascular network complexity in

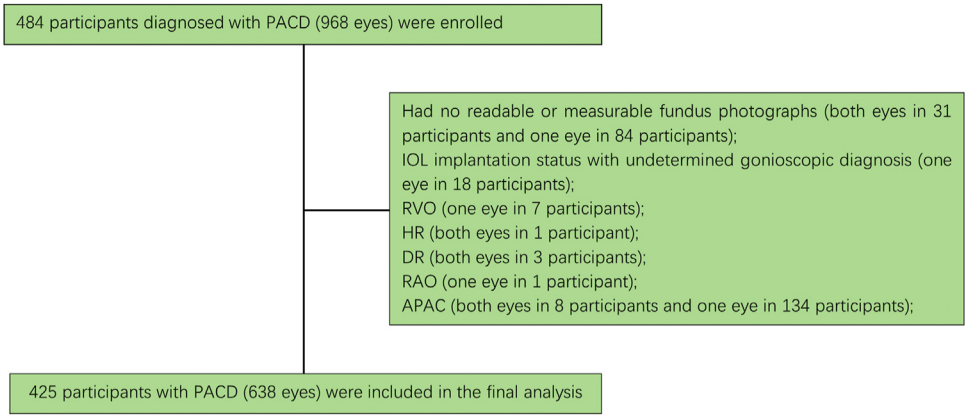

Figure 2. Flowchart of enrollment of the study participants. APAC = acute primary angle closure; DR = diabetic retinopathy; HR = hypertensive retinopathy; IOL = intraocular lens; PACD = primary angle-closure disease; RAO = retinal artery occlusion; RVO = retinal vein occlusion.

advanced disease. For branching angle parameters, eyes with PACG showed reduced angular asymmetry ($P < 0.001$ for artery and vein), decreased branching angles ($P < 0.001$ for artery and vein), and lower asymmetry ratios (AR, $P < 0.001$ for artery and $P = 0.007$ for vein). Junctional exponent deviation measurements did not differ significantly between the 3 groups (all $P > 0.05$).

Factors Associated with GON in PACD

Table 3 shows the results of mixed-effects logistic regression analyses of factors associated with GON in PACD. In the multivariable model, increased IOP (OR = 2.44 per 1 mmHg increase, 95% CI: 1.71−3.48, $P < 0.001$) remained strongly associated with GON. Among vascular parameters, decreased arteriolar curve tortuosity (OR = 0.12, 95% CI: 0.03−0.45, $P = 0.002$), lower arteriolar FD (OR = 0.08, 95% CI: 0.01−0.75, $P = 0.027$), decreased arteriolar branching angle (OR = 0.16, 95% CI: 0.05−0.56, $P = 0.004$), and reduced AR (OR = 0.10, 95% CI: 0.03−0.35, $P < 0.001$ for artery and OR = 0.25, 95% CI: 0.08−0.83, $P = 0.023$ for vein) were independently associated with the presence of GON.

Table 1. Demographic and Ocular Biometric Characteristics of the Participants in the PACS, PAC, and PACG Groups

Parameter	1 = PACS (n = 201)	2 = PAC (n = 57)	3 = PACG (n = 167)	P Value
Age (IQR), yrs	66.0 (61.0−70.0)	66.4 (60.0−70.0)	66.0 (59.0−72.0)	0.815*
Sex				
Male (%)	46 (22.9)	12 (21.1)	56 (33.5)	**0.041**†
Female (%)	155 (77.1)	45 (78.9)	111 (66.5)	
Hypertension				
No (%)	169 (84.1)	49 (86.0)	145 (86.8)	0.753†
Yes (%)	32 (15.9)	8 (14.0)	22 (13.2)	
Diabetes				
No (%)	192 (95.5)	54 (94.7)	155 (92.8)	0.529†
Yes (%)	9 (4.5)	3 (5.3)	12 (7.2)	
Hyperlipidemia				
No (%)	189 (94.0)	52 (91.2)	154 (92.2)	0.687†
Yes (%)	12 (6.0)	5 (8.8)	13 (7.8)	
PVA (IQR)	0.22 (0.10−0.40)	0.22 (0.10−0.40)	0.30 (0.15−0.70)	**<0.001***
AK (IQR), diopters	44.44 (43.51−45.41)	44.45 (43.29−45.45)	44.70 (43.29−45.46)	0.803*
IOP (IQR), mmHg	15.0 (13.0−16.7)	16.0 (13.8−18.0)	17.0 (14.0−22.0)	**<0.001***
VCDR (IQR)	0.30 (0.30−0.50)	0.30 (0.40−0.60)	0.77 (0.60−0.90)	**<0.001***
CCT (IQR), μm	527.0 (506.0−555.0)	533.5 (512.0−561.3)	526.0 (497.0−554.0)	0.412*
Central ACD (IQR), mm	2.36 (2.23−2.55)	2.27 (2.10−2.54)	2.38 (2.22−2.55)	0.103*
LT (IQR), mm	4.97 (4.82−5.22)	4.96 (4.78−5.31)	4.94 (4.73−5.17)	0.226*
AL (IQR), mm	22.45 (21.93−22.99)	22.61 (22.14−23.06)	22.55 (22.09−23.01)	0.458*

ACD = anterior chamber depth; AK = average keratometry; AL = axial length; CCT = central corneal thickness; IOP = intraocular pressure; IQR = interquartile range; LT = lens thickness; PAC = primary angle closure; PACG = primary angle-closure glaucoma; PACS = primary angle-closure suspect; PVA = presenting visual acuity; VCDR = vertical cup disc ratio.
Bold values indicate statistical significance at $P < 0.05$.
*Kruskal−Wallis test.
†χ^2 test.

Table 2. Retinal Vascular Parameters in PACS, PAC, and PACG Groups

Category	Parameter	PACS (n = 305)	PAC (n = 91)	PACG (n = 242)	P*	P†	Effect Size (d)
Caliber	LDR (artery)	13.04 (11.68–16.05)	13.30 (11.62–17.93)	17.10 (13.37–22.11)	0.795	**<0.001**	**0.610**
	LDR (vein)	11.65 (11.04–13.52)	11.96 (11.13–13.50)	13.32 (11.91–17.22)	0.935	**<0.001**	**0.486**
	AVRQ4	0.77 (0.71–0.82)	0.76 (0.71–0.81)	0.73 (0.66–0.78)	0.915	**<0.001**	**−0.487**
Tortuosity	Tortuosity (artery)	1.08 (1.08–1.09)	1.08 (1.08–1.09)	1.08 (1.07–1.08)	0.983	**0.018**	**−0.258**
	Tortuosity (vein)	1.08 (1.08–1.09)	1.08 (1.08–1.09)	1.08 (1.08–1.09)	0.985	0.079	-
	Curve tortuosity (artery)	0.11 (0.11–0.12)	0.11 (0.11–0.13)	0.11 (0.10–0.12)	0.768	**<0.001**	**−0.309**
	Curve tortuosity (vein)	0.12 (0.11–0.13)	0.12 (0.11–0.13)	0.12 (0.11–0.13)	0.617	0.738	-
Complexity	FD (artery)	1.50 (1.44–1.54)	1.48 (1.39–1.53)	1.44 (1.37–1.50)	0.647	**<0.001**	**−0.610**
	FD (vein)	1.55 (1.51–1.58)	1.56 (1.51–1.57)	1.51 (1.46–1.55)	0.980	**<0.001**	**−0.569**
Branching angle parameters	Angular asymmetry (artery)	42.66 (39.17–45.72)	43.21 (39.27–45.53)	39.86 (35.79–44.13)	0.322	**<0.001**	**−0.330**
	Angular asymmetry (vein)	41.11 (38.31–44.26)	40.81 (37.42–44.04)	39.28 (35.73–42.67)	0.992	**<0.001**	**−0.378**
	Branching coefficient (artery)	1.24 (1.17–1.32)	1.23 (1.15–1.30)	1.26 (1.19–1.34)	0.637	0.402	-
	Branching coefficient (vein)	1.18 (1.13–1.28)	1.17 (1.12–1.28)	1.20 (1.13–1.28)	0.765	0.472	-
	Branching angle (artery)	45.39 (43.88–46.64)	45.09 (43.47–46.97)	44.17 (41.79–45.79)	0.996	**<0.001**	**−0.471**
	Branching angle (vein)	46.71 (45.52–47.71)	46.42 (44.86–47.14)	45.98 (44.33–47.23)	0.159	**<0.001**	**−0.410**
	AR (artery)	2.12 (1.78–2.42)	2.17 (1.89–2.49)	1.94 (1.62–2.26)	0.825	**<0.001**	**−0.325**
	AR (vein)	2.54 (2.21–2.92)	2.54 (2.27–3.00)	2.38 (2.04, 2.83)	0.638	**0.007**	**−0.259**
	JED (artery)	−0.04 (−0.13 to 0.06)	−0.04 (−0.10 to 0.08)	−0.09 (−0.18 to 0.02)	0.575	0.104	-
	JED (vein)	0.035 (−0.03 to 0.114)	0.044 (−0.024 to 0.101)	0.014 (−0.056 to 0.115)	0.984	0.974	-

AR = asymmetry ratio; AVRQ4 = artery-to-vein ratio from quantile 4; FD = fractal dimension; JED = junctional exponent deviation; PAC = primary angle closure; PACG = primary angle-closure glaucoma; PACS = primary angle closure suspect; LDR = length diameter ratio.
Effect size (d): Cohen's d for PACG vs. PACS, reported only where P2 < 0.05.
Bold values indicate statistical significance at $P < 0.05$.
*P represents the P value for PAC vs. PACS comparisons.
†P represents the P value for PACG vs. PACS comparisons.

Table 3. Factors Associated with Glaucomatous Optic Neuropathy

Variable	Univariable Logistic Regression		Multivariable Logistic Regression		
	OR (95% CI)	P *Value*	*OR (95% CI)*	P *Value*	*VIF*
Age, per 10 yrs older	1.39 (0.95, 2.03)	0.087			
Sex, female	0.46 (0.21, 1.01)	0.053			
Hypertension, yes	0.84 (0.33, 2.14)	0.721			
Diabetes, yes	1.71 (0.43, 6.84)	0.446			
IOP, per 1 mmHg increase	1.86 (1.53, 2.27)	**<0.001**	2.44 (1.71–3.48)	**<0.001**	1.60
ACD, per 1 mm increase	1.82 (0.85, 3.91)	0.125			
LT, per 1 mm increase	0.56 (0.27, 1.20)	0.135			
AL, per 1 mm increase	1.15 (0.84, 1.57)	0.387			
LDR (artery), per 1 SD increase	81.57 (19.28, 345.16)	**<0.001**	1.18 (0.21–6.56)	0.846	3.02
LDR (vein), per 1 SD increase	23.57 (6.92, 80.26)	**<0.001**	-	-	
AVRQ4, per 1 SD increase	0.39 (0.25, 0.62)	**<0.001**	0.32 (0.10–1.01)	0.053	1.33
Tortuosity (artery), per 1 SD increase	0.56 (0.38, 0.82)	**0.003**	1.00 (0.21–4.76)	0.993	1.32
Curve tortuosity (artery), per 1 SD increase	0.65 (0.49, 0.85)	**0.002**	0.12 (0.03–0.45)	**0.002**	1.90
FD (artery), per 1 SD increase	0.02 (0.02, 0.02)	**<0.001**	0.08 (0.01–0.75)	**0.027**	3.28
FD (vein), per 1 SD increase	0.03 (0.01, 0.11)	**<0.001**	-	-	
Angular asymmetry (artery), per 1 SD increase	0.49 (0.34, 0.72)	**<0.001**	2.41 (0.78–7.40)	0.126	1.57
Angular asymmetry (vein), per 1 SD increase	0.42 (0.24, 0.74)	**0.003**	0.82 (0.19–3.46)	0.785	1.78
Branching angle (artery), per 1 SD increase	0.11 (0.05, 0.26)	**<0.001**	0.16 (0.05–0.56)	**0.004**	1.37
Branching angle (vein), per 1 SD increase	0.55 (0.41, 0.74)	**<0.001**	0.85 (0.36–1.98)	0.700	1.36
AR (artery), per 1 SD increase	0.18 (0.08, 0.39)	**<0.001**	0.10 (0.03–0.349)	**<0.001**	1.51
AR (vein), per 1 SD increase	0.58 (0.42, 0.79)	**0.001**	0.25 (0.08–0.83)	**0.023**	1.90

ACD = anterior chamber depth; AL = axial length; AR = asymmetry ratio; AVRQ4 = artery-to-vein ratio from quantile 4; CI = confidence interval; FD = fractal dimension; IOP = intraocular pressure; LDR = length diameter ratio; LT = lens thickness; OR = odds ratio; SD = standard deviation; VIF = variance inflation factor.
Bold values indicate statistical significance at $P < 0.05$.

The final multivariable model combining IOP and vascular parameters demonstrated excellent discriminative ability for GON (area under the receiver operating characteristic curve = 0.769, 95% CI: 0.730–0.808), significantly outperforming the baseline model using IOP alone (area under the receiver operating characteristic curve = 0.671, 95% CI: 0.626–0.716; DeLong test $P < 0.001$) (Fig 3).

Discussion

The association between retinal hemodynamics and GON has been a longstanding area of interest in glaucoma research.[3,15,16] Alterations in vascular geometry represent a crucial aspect of hemodynamic changes and may serve as a significant indicator of underlying shifts in retinal blood flow and tissue perfusion under pathological conditions.[9,10,16] Given that no study has reported retinal geometric alterations in PACD, we conducted this study to investigate the differences in quantifiable vascular geometric parameters among various stages of PACD as well as their association with the presence of GON.

One key finding of our study was the absence of significant differences in retinal vascular parameters between the PACS and PAC groups. This observation suggests that retinal vascular parameters remain stable in the early stages of PACD, despite intermittent IOP elevations. This stability may indicate preservation of retinal blood flow, possibly mediated by autoregulatory mechanisms.[17–20] Previous studies have demonstrated that retinal autoregulation remains functional during experimental IOP elevations of up to 29 mmHg.[20] Furthermore, the characteristic intermittent and mild IOP elevations in patients with PAC may be insufficient to induce significant vascular parameter alterations comparable to those observed in advanced GON.[21–25] This pattern parallels the stability of optic disc parameters between these stages, suggesting that both structural disc changes and vascular alterations may occur relatively late in the disease process, potentially after autoregulatory mechanisms are overwhelmed by sustained pressure-related stress.

Comparing eyes with PACG with PACS revealed significant reductions in several parameters, characterized by decreased vessel complexity (FD), reduced tortuosity, and altered branching angle parameters, with moderate to large effect sizes. These changes suggest that substantial vascular remodeling occurred in eyes with GON. However, the cross-sectional nature of this study precludes definitive conclusions regarding the causal relationship between vascular alterations and the development of GON. Therefore, whether vascular insufficiency precedes GON or if these changes are secondary to tissue loss and reduced metabolic demand remains unclear. Longitudinal studies are crucial for elucidating the temporal sequence and causal mechanisms underlying PACD progression.

Recent advances in OCT angiography have enabled detailed visualization of microvascular alterations in PACD, such as reduced vessel density and capillary dropout in the peripapillary and macular regions.[24,25] Although OCT angiography-based metrics provide a high-resolution

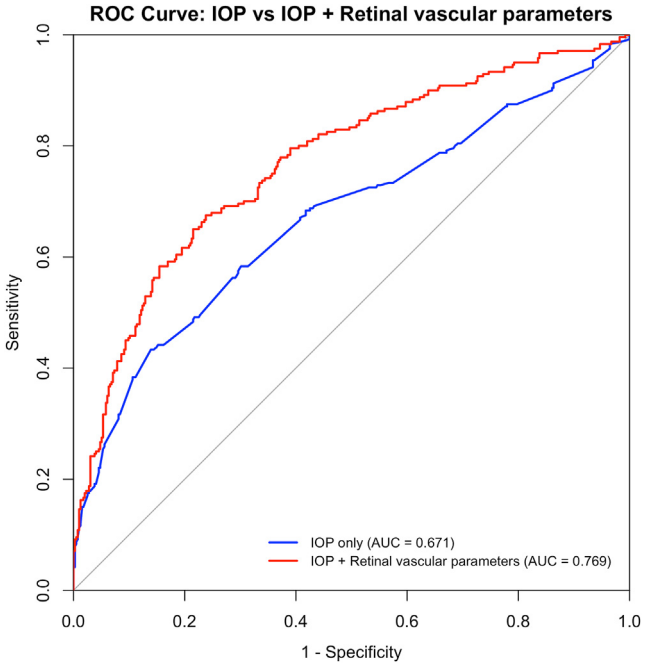

Figure 3. Receiver operating characteristic curves comparing predictive models for glaucomatous optic neuropathy in primary angle-closure disease. The blue line represents the model incorporating only IOP as a predictor (AUC = 0.671). The red line represents the multivariable model combining IOP with retinal vascular parameters (AUC = 0.769). The combined model demonstrates significantly improved discriminative ability (DeLong test, $P < 0.001$). AUC = area under the receiver operating characteristic curve; IOP = intraocular pressure; ROC = receiver operating characteristic.

assessment of current perfusion status, they require costly equipment and standardized imaging protocols. In contrast, retinal vascular parameters derived from fundus photographs offer a cost-effective alternative that captures long-term structural vascular remodeling rather than momentary perfusion states. The 2 approaches may offer complementary insights into vascular dysfunction in PACD, and future studies could explore their combined diagnostic potential.

The hemodynamic implications behind these changes in retinal vascular parameters detected from our study are complex. Reduced tortuosity stands for straighter vessels, which typically enhance blood flow efficiency by reducing resistance.[26] Paradoxical effects have been observed in certain pathological conditions, such as diabetic retinopathy, where reduced tortuosity is correlated with diminished blood flow and compromised tissue perfusion.[16,26] Similarly, lower FD suggests a simpler, less dense vascular network. These changes may indicate increased vascular resistance and impaired blood flow or, alternatively, represent the adaptation of blood flow redistribution to ischemic tissues.[9,27] Notably, reductions in these vessel geometric parameters do not universally signify pathological changes, emphasizing the need for cautious interpretation within the specific disease context.

Our multivariable logistic regression analysis revealed that multiple vascular parameters remained independently associated with GON after adjusting for IOP. The substantial associations between GON and reduced arteriolar curve tortuosity, FD, branching angle, and AR suggest these parameters may reflect discrete components of vascular dysfunction in PACD pathophysiology. Importantly, incorporation of these vascular parameters significantly enhanced the model's discriminative capacity for GON detection compared to IOP alone, underscoring their potential utility as clinical biomarkers.

Our study also demonstrates a predominance of arteriolar rather than venular alterations associated with GON in PACD. This discrepancy may be attributed to fundamental differences in hemodynamic roles and vascular responsiveness. Arterioles serve as the primary resistance vessels in the retinal circulation and are actively involved in blood flow autoregulation to meet local metabolic demands.[28–30] Under chronic ischemic conditions or elevated IOP, autoregulatory failure of arterioles may occur, leading to structural remodeling such as reduced tortuosity and altered branching geometry, which were captured by the parameters assessed in our previous studies.[11,31–34] In contrast, venules primarily function as low-resistance capacitance vessels with limited capacity for active regulation, and their structural characteristics are generally more stable and less responsive to transient or localized ischemic stress. This mechanistic distinction may underlie the observed arteriolar-venular asymmetry in their associations with GON.

The strength of our study lies in providing potential applications of retinal vascular mapping in angle-closure disease, where certain parameters, such as those reflecting arteriolar complexity and branching patterns, may serve as potential indicators of glaucomatous progression in PACD. Future longitudinal studies are needed to validate their predictive value and explore their utility in clinical decision-making, such as risk stratification or monitoring therapeutic response.

Several limitations of this study warrant consideration. First, the cross-sectional design limits the ability to establish causal relationships between the alteration of retinal vessel geometric parameters and PACD progression. Second, the study population was recruited from a single hospital and, therefore, may not be fully representative of the general PACD population. Third, although our study controlled for some factors, such as age and systemic conditions, other potential confounders, such as medication use, smoking status, or other ocular conditions, may not have been fully accounted for. Lastly, although we excluded eyes with a history of acute PAC to minimize physiologic confounding from acute and transient vascular perturbations, this exclusion limits the interpretation of our findings to acute angle closure. Future studies should consider dedicated subgroup analyses comparing acute and chronic angle closure to elucidate the dynamic vascular responses associated with acute IOP spikes and their potential impact on long-term retinal vascular geometry.

In conclusion, this study revealed that retinal vascular parameters remain relatively stable in the early stages of PACD but show significant alterations in the advanced stage of PACG with established GON. Higher IOP, lower arteriolar branching angle, curve tortuosity, and FD, as well as lower AR in artery and vein, were significantly associated with the presence of GON. Although these findings offer new insights into the vascular changes accompanying disease severity, longitudinal studies are needed to determine their prognostic value and clinical utility in managing PACD.

Data Sharing

The authors declare that all data supporting the findings of this study are available within the paper. The data have not been made publicly available, and restrictions apply to their use. All requests would require evaluation on an individual basis and can be made by contacting drzhangye@mail.ccmu.edu.cn, wningli@vip.163.com.

Footnotes and Disclosures

Originally received: March 4, 2025.
Final revision: May 19, 2025.
Accepted: June 2, 2025.
Available online: June 9, 2025. Manuscript no. XOPS-D-25-00139.

[1] Beijing Tongren Eye Center, Beijing Key Laboratory of Ophthalmology and, Visual Science, Beijing Tongren Hospital, Capital Medical University, Beijing, China.

[2] Beijing Institute of Ophthalmology, Beijing, China.

[3] Ningxia Eye Hospital, People's Hospital of Ningxia Hui Autonomous Region, Yinchuan, China.

[4] Qingdao University, Qingdao, China.

[5] Centre for Eye and Vision Research (CEVR), The Hong Kong Polytechnic University, Kowloon, Hong Kong SAR, China.

[6] Linfen Yaodu Eye Hospital, Linfen, Shanxi, China.

*J.W. and S.H. contributed equally to this work and should be listed as co-first authors.

Disclosure(s):

All authors have completed and submitted the ICMJE disclosures form.

The authors have no proprietary or commercial interest in any materials discussed in this article.

This work was supported by the General Program of National Natural Science Foundation of China (grant number: 82371050). The funding organization had no role in the study design; collection, analysis, and interpretation of data; writing of the report; and decision to submit the article for publication.

HUMAN SUBJECTS: Human subjects were included in this study. The Institutional Review Board of Beijing Tongren Hospital waived the need for informed consent and granted ethical approval for the study protocol (TREC2024-KY064). This study was conducted in accordance with the principles of the Declaration of Helsinki.

No animal subjects were used in this study.

Author Contributions:

Conception and design: Wang, Zhang

Data collection: Wang, Han, Mou, Tang, Guo, Wang, Zhang

Analysis and interpretation: Wang, Shi, He, Zhang

Obtained funding: Zhang

Overall responsibility: Wang, Zhang

Abbreviations and Acronyms:
AR = asymmetry ratio; **CI** = confidence interval; **FD** = fractal dimension; **GON** = glaucomatous optic neuropathy; **IOP** = intraocular pressure; **OR** = odds ratio; **PAC** = primary angle closure; **PACD** = primary angle-closure disease; **PACG** = primary angle closure glaucoma; **PACS** = primary angle closure suspect.

Keywords:
Primary angle closure disease, Retinal vascular fingerprints, Glaucomatous optic neuropathy.

Correspondence:
Ning Li Wang, MD, PhD, Beijing Institute of Ophthalmology, Beijing Tongren Eye Center, Beijing Key Laboratory of Ophthalmology and Visual Sciences, Beijing Tongren Hospital Capital Medical University, No. 1 dong Jiao Min Xiang Street, Dongcheng District, Beijing 100730, China. E-mail: wningli@vip.163.com; and Ye Zhang, MD, Beijing Tongren Eye Center, Beijing Key Laboratory of Ophthalmology and Visual Science Beijing Tongren Hospital, Capital Medical University, No. 1 dong Jiao Min Xiang Street, Dongcheng District, Beijing 100730, China. E-mail: drzhangye@mail.ccmu.edu.cn.

References

1. Weinreb RN, Aung T, Medeiros FA. The pathophysiology and treatment of glaucoma: a review. *JAMA*. 2014;311:1901–1911.

2. Jonas JB, Budde WM. Diagnosis and pathogenesis of glaucomatous optic neuropathy: morphological aspects. *Prog Retin Eye Res*. 2000;19:1–40.

3. Flammer J, Orgül S, Costa VP, et al. The impact of ocular blood flow in glaucoma. *Prog Retin Eye Res*. 2002;21:359–393.
4. Hafez AS, Lesk MR. Role of ocular blood flow in the pathogenesis of glaucoma. In: *Glaucoma*. Philadelphia, PA: Elsevier; 2015:88–97.
5. Costa VP, Harris A, Anderson D, et al. Ocular perfusion pressure in glaucoma. *Acta Ophthalmol*. 2014;92:e252–e266.
6. Foster PJ, Buhrmann R, Quigley HA, Johnson GJ. The definition and classification of glaucoma in prevalence surveys. *Br J Ophthalmol*. 2002;86:238–242.
7. Zheng Y, Cheung N, Aung T, et al. Relationship of retinal vascular caliber with retinal nerve fiber layer thickness: the Singapore Malay Eye Study. *Invest Ophthalmol Vis Sci*. 2009;50:4091–4096.
8. Su DH, Wong TY, Liu E, et al. Retinal vascular caliber and primary glaucoma subtypes in Asians. *Investig Ophthalmol Vis Sci*. 2010;51:2684.
9. Wu R, Cheung CY, Saw SM, et al. Retinal vascular geometry and glaucoma: the Singapore Malay Eye Study. *Ophthalmology*. 2013;120:77–83.
10. Tham YC, Cheng CY, Zheng Y, et al. Relationship between retinal vascular geometry with retinal nerve fiber layer and ganglion cell-inner plexiform layer in nonglaucomatous eyes. *Invest Ophthalmol Vis Sci*. 2013;54:7309–7316.
11. Mitchell P, Leung H, Wang JJ, et al. Retinal vessel diameter and open-angle glaucoma: the blue mountains eye study. *Ophthalmology*. 2005;112:245–250.
12. Amerasinghe N, Aung T, Cheung N, et al. Evidence of retinal vascular narrowing in glaucomatous eyes in an Asian population. *Invest Ophthalmol Vis Sci*. 2008;49:5397–5402.
13. Patton N, Aslam TM, MacGillivray T, et al. Retinal image analysis: concepts, applications and potential. *Prog Retin Eye Res*. 2006;25:99–127.
14. Shi D, Lin Z, Wang W, et al. A deep learning system for fully automated retinal vessel measurement in high throughput image analysis. *Front Cardiovasc Med*. 2022;9:823436.
15. Sehi M, Goharian I, Konduru R, et al. Retinal blood flow in glaucomatous eyes with single-hemifield damage. *Ophthalmology*. 2014;121:750–758.
16. Jmor F, Chen JC. Retinal vascular implications of ocular hypertension. In: Lanza M, ed. *Ocular Hypertension – the Knowns and Unknowns*. London: IntechOpen; 2021.
17. Riva CE, Grunwald JE, Petrig BL. Autoregulation of human retinal blood flow. An investigation with laser Doppler velocimetry. *Invest Ophthalmol Vis Sci*. 1986;27:1706–1712.
18. Arciero J, Harris A, Siesky B, et al. Theoretical analysis of vascular regulatory mechanisms contributing to retinal blood flow autoregulation. *Invest Ophthalmol Vis Sci*. 2013;54:5584–5593.
19. Pournaras CJ, Rungger-Brändle E, Riva CE, et al. Regulation of retinal blood flow in health and disease. *Prog Retin Eye Res*. 2008;27:284–330.
20. Grunwald JE, Riva CE, Stone RA, et al. Retinal autoregulation in open-angle glaucoma. *Ophthalmology*. 1984;91:1690–1694.
21. Zhu L, Zong Y, Yu J, et al. Reduced retinal vessel density in primary angle closure glaucoma: a quantitative study using optical coherence tomography angiography. *J Glaucoma*. 2018;27:322–327.
22. Ma ZW, Qiu WH, Zhou DN, et al. Changes in vessel density of the patients with narrow antenior chamber after an acute intraocular pressure elevation observed by OCT angiography. *BMC Ophthalmol*. 2019;19:132.
23. Lin B, Zuo C, Gao X, et al. Quantitative measurements of vessel density and blood flow areas primary angle closure diseases: a study of optical coherence tomography angiography. *J Clin Med*. 2022;11:4040.
24. Sener H, Evereklioglu C, Horozoglu F, Sener ABG. Optic nerve head vessel density using OCTA in patients with primary angle closure disease: a systematic review and network meta-analysis. *Photodiagn Photodyn Ther*. 2023;41:103209.
25. Rao HL, Pradhan ZS, Weinreb RN, et al. Vessel density and structural measurements of optical coherence tomography in primary angle closure and primary angle closure glaucoma. *Am J Ophthalmol*. 2017;177:106–115.
26. Choi JM, Kim SM, Bae YH, Ma DJ. A study of the association between retinal vessel geometry and optical coherence tomography angiography metrics in diabetic retinopathy. *Invest Ophthalmol Vis Sci*. 2021;62:14.
27. Koh V, Cheung CY, Zheng Y, et al. Relationship of retinal vascular tortuosity with the neuroretinal rim: the Singapore Malay eye study. *Invest Ophthalmol Vis Sci*. 2010;51:3736–3741.
28. Fortune B, Cull G, Reynaud J, et al. Relating retinal ganglion cell function and retinal nerve fiber layer (RNFL) retardance to progressive loss of RNFL thickness and optic nerve axons in experimental glaucoma. *Invest Ophthalmol Vis Sci*. 2015;56:3936–3944.
29. Casson RJ, Chidlow G, Crowston JG, et al. Retinal energy metabolism in health and glaucoma. *Prog Retin Eye Res*. 2021;81:100881.
30. Rombaut A, Brautaset R, Williams PA, Tribble JR. Glial metabolic alterations during glaucoma pathogenesis. *Front Ophthalmol (Lausanne)*. 2023;3:1290465.
31. Carlson BE, Arciero JC, Secomb TW. Theoretical model of blood flow autoregulation: roles of myogenic, shear-dependent, and metabolic responses. *Am J Physiol Heart Circ Physiol*. 2008;295:H1572–H1579.
32. Wang S, Xu L, Wang Y, et al. Retinal vessel diameter in normal and glaucomatous eyes: the Beijing eye study. *Clin Exp Ophthalmol*. 2007;35:800–807.
33. Hall JK, Andrews AP, Walker R, Piltz-Seymour JR. Association of retinal vessel caliber and visual field defects in glaucoma. *Am J Ophthalmol*. 2001;132:855–859.
34. Kawasaki R, Wang JJ, Rochtchina E, et al. Retinal vessel caliber is associated with the 10-year incidence of glaucoma: the Blue Mountains Eye Study. *Ophthalmology*. 2013;120:84–90.